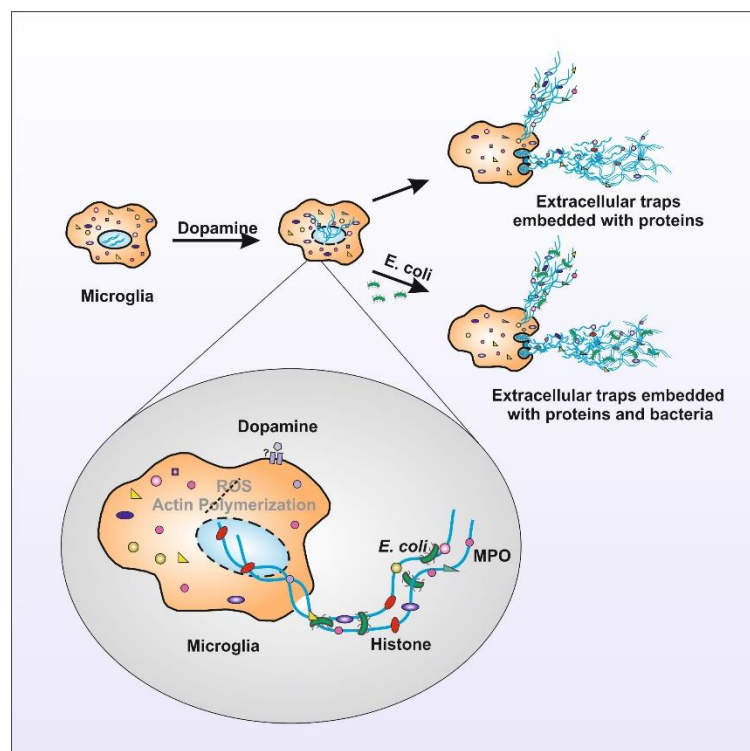


# Dopamine induces functional extracellular traps in microglia

## 4.1 ABSTRACT

Dopamine (DA) is central to neurological functions like motivation, movement and reward (Klein et al. 2019). While its role in diseases like Parkinson's, Alzheimer's and schizophrenia are well studied, its role in regulating immune functions have just started to unfold. DA receptors are present on almost all immune cells and they regulate innate and adaptive immunity (Matt and Gaskill 2020). We have investigated the role of DA in the formation of extracellular traps (ETs) in microglia. We report that DA can induce ETs in BV2 microglia cell line and primary adult human microglia. ETs are composed of decondensed chromatin and are embedded with proteins including antimicrobial proteins like myeloperoxidase and histone. We confirmed ETs formation by staining them with DAPI, myeloperoxidase and/or DNA/Histone H1. The presence of traps in culture supernatant was confirmed by measuring SYTOX Green absorbance. To check for the mechanism of ETs formation by BV2 cells, we performed MTT assay and treated cells with N-acetyl L-cysteine or cytochalasin D. We saw that the traps were formed independent of cell death, reactive oxygen species (ROS) and actin polymerization. We further confirmed that DA induced microglia traps are functional as they were able to trap FITC tagged *Escherichia coli*. Lastly we checked the presence of microglia ETs in *Glioblastoma multiforme* tissues as recently glioma cells have been reported to secrete DA and possess DA receptors (Caragher et al. 2019). We confirmed and quantified the traps present in GBM by an unbiased algorithm. Our findings demonstrate that DA may play a significant role in sterile neuro-inflammation by inducing microglia ETs.



## 4.2 INTRODUCTION

In 2004 Zychlinsky *et al.* discovered that neutrophils can control the spread of pathogens by forming extracellular traps (ETs), also referred to as neutrophil extracellular traps (NETs). ETs are composed of nuclear or mitochondrial DNA (Brinkmann, Reichard *et al.* 2004, Pocock and Kettenmann 2007, Lood, Blanco *et al.* 2016). ETs are decorated with multiple antimicrobial proteins like myeloperoxidase and neutrophil elastase (Dwyer, Shan *et al.* 2014, Delgado-Rizo, Martínez-Guzmán *et al.* 2017, Papayannopoulos 2017) and are capable of trapping and killing bacteria (Brinkmann, Reichard *et al.* 2004), fungi (Urban, Reichard *et al.* 2006), parasites (Abi Abdallah, Lin *et al.* 2012) and viruses (Saitoh, Komano *et al.* 2012). It is now known that innate immune cells such as monocytes (Webster, Daigneault *et al.* 2010), macrophages (Chow, von Köckritz-Blickwede *et al.* 2010), eosinophils (Yousefi, Gold *et al.* 2008), basophils (Schorn, Janko *et al.* 2012, Morshed, Hlushchuk *et al.* 2014) and mast cells (Möllerherm, von Köckritz-Blickwede *et al.* 2016) can also form ETs.

Two mechanisms are proposed for NETs formation (NETosis): suicidal or lytic NETosis and vital or non-lytic NETosis (Fuchs, Abed *et al.* 2007, Pilszczek, Salina *et al.* 2010, Yipp, Petri *et al.* 2012, Papayannopoulos 2017, Yousefi, Stojkov *et al.* 2019). In lytic NETosis decondensed chromatin is released with the permeabilization of nuclear envelope and cell membrane leading to immediate cell death (Fuchs, Brill *et al.* 2010, Papayannopoulos 2017). In non-lytic NETosis, decondensed chromatin is released in vesicles along with granules containing antimicrobial proteins without compromising the cell membrane and cells continue to function normally (Yipp, Petri *et al.* 2012, Papayannopoulos 2017). Yousefi *et al.* first reported that viable neutrophils can produce NETs composed of mitochondrial DNA rather than nuclear DNA (Yousefi, Mihalache *et al.* 2009). Lytic NETosis is most studied and is reactive oxygen species (ROS) dependent (Fuchs, Brill *et al.* 2010, Papayannopoulos 2017). The precise mechanism behind NETosis is still not known and is a topic of intense research. Stimuli like PMA (Phorbol 12-myristate 13-acetate), LPS (Lipopolysaccharides), platelets, GM-CSF (Granulocyte-macrophage colony-stimulating factor), oxidized low density lipoprotein, and statins induce ETs (Chow, von Köckritz-Blickwede *et al.* 2010, Caudrillier, Kessenbrock *et al.* 2012, Delgado-Rizo, Martínez-Guzmán *et al.* 2017, Wang, Wang *et al.* 2019). Pathologic conditions such as hyperglycemia impair the ability of neutrophils to form NETs and reduce their antimicrobial properties (Joshi, Lad *et al.* 2013).

ETs play an important role in immune surveillance and pathogen clearance, but their persistence post infection makes them inflammatory and harmful (Pocock and Kettenmann 2007, Hakkim, Fürnrohr *et al.* 2010, Wright, Gibson *et al.* 2016, Papayannopoulos 2017). ETs contribute to tissue damage (Villanueva, Yalavarthi *et al.* 2011, Saffarzadeh, Juenemann *et al.* 2012, Czaikoski, Mota *et al.* 2016), vaso-occlusion (Fuchs, Brill *et al.* 2010, Martinod, Demers *et al.* 2013), sterile inflammation (Warnatsch, Ioannou *et al.* 2015), cancer (Demers, Krause *et al.* 2012, Cedervall, Zhang *et al.* 2015, Guglietta, Chiavelli *et al.* 2016), rheumatoid arthritis (Khandpur, Carmona-Rivera *et al.* 2013) and systemic lupus erythematosus (SLE) (Garcia-Romo, Caielli *et al.* 2011, Yu and Su 2013). Calcium phosphate based mineralo-organic particles, some of which are spontaneously generated in the body, induce NETs that leads to inflammation through high-mobility group protein B1 (HMGB1) (Peng, Liu *et al.* 2017). It is critical to understand the regulation of formation and disassembly of ETs for therapeutic interventions.

Innate immune cells form ETs; macrophages forming ETs is actively studied. Human peripheral-blood monocytes (Jönsson, Bylund *et al.* 2013, Halder, Abdelfatah *et al.* 2016), human monocyte-derived macrophages (Wong and Jacobs 2013), human alveolar macrophages (King, Sharma *et al.* 2015), THP-1 monocytic cell line (Shen, Tang *et al.* 2016), murine peritoneal macrophages (Chow, von Köckritz-Blickwede *et al.* 2010), and rat macrophages (Bryukhin and Shopova 2015) form ETs, referred to as macrophage extracellular traps (METs) (Doster, Rogers

et al. 2017). Until recently ETs formation by microglia was not reported (Wang, Wang et al. 2019). Microglia are resident myeloid cells of the central nervous system (CNS). They play critical role in clearing debris and maintaining homeostasis in the CNS (Li and Barres 2018). These roles of microglia are regulated by multiple factors including neurotransmitters (Pocock and Kettenmann 2007, Yoshioka, Sugino et al. 2016, Fan, Chen et al. 2018). Dopamine (DA) is one of the key neurotransmitters in the brain. It controls a variety of functions including locomotor activities, emotion, and cognition (Beninger 1983, Ferreri, Mas-Herrero et al. 2019, Ott and Nieder 2019). DA is also important for immunity within the CNS and in the body (Arreola, Alvarez-Herrera et al. 2016, Fan, Chen et al. 2018). Recently Caragher *et al.* reported that Glioblastoma cells express dopamine receptor 2 (DR2) and can synthesize and secrete DA (Caragher, Shireman et al. 2019). This affects GBM metabolism and may enhance tumor growth. Activation of DR2 increases spheroid forming capacity of GBM cells (Caragher, Shireman et al. 2019, Weissenrieder, Reed et al. 2019). These findings indicate a possible role of DA in the regulation of GBM.

Based on these observations we investigated whether DA can induce ETs in BV2 microglia cell line and primary adult human microglia. We explored the basic mechanism of microglia ETs formation, functionality of these traps and their presence in GBM.

## 4.3 MATERIALS AND METHODS

### 4.3.1 CELL CULTURE

The murine microglial cell line BV2 were a kind gift from Dr. Anirban Basu (National Brain Research Centre, Gurgaon). The cells were cultured in DMEM, high glucose medium, supplemented with 10% FBS and 1 % antibiotic antimycotic stabilized solution (Himedia). The cells were grown in 96-well plate or in chamber slides as required. They were incubated at 37°C with 5% CO<sub>2</sub> for 24 hours (Eppendorf-170 S, Incubator). The confluent microplate or chamber slides were then used for experiments.

### 4.3.2 PRIMARY HUMAN MICROGLIA ISOLATION

Ethical clearance for acquiring tissues was taken from the Institute ethics committees of Indian Institute of Technology Jodhpur and All India Institute of Medical Science (AIIMS) Jodhpur. Informed consent was acquired for the use of tissue samples for experiments from human participants. A protocol for isolating primary microglia from adult human brain tissues was developed (Agrawal, Saxena et al. 2020). Brain tissue was transported to lab in artificial cerebrospinal fluid (acsf) (2mM - CaCl<sub>2</sub>-2H<sub>2</sub>O, 10mM - Glucose, 3mM - KCl, 26mM - NaHCO<sub>3</sub>, 2.5mM - NaH<sub>2</sub>PO<sub>4</sub>, 1mM - MgCl<sub>2</sub>-6H<sub>2</sub>O, 202mM - Sucrose) on ice. Tissue was washed for 5 minutes with acsf and then 5 minutes with PBS. Tissue was minced into small pieces and was incubated in 10ml trypsin for 25 minutes at 37°C. 10 ml media (DMEM/F12 with glutamine, 1% penicillin-streptomycin, 20% L929 supernatant, 10% FBS) was added and tissue was centrifuged at 2000xg for 10 minutes at 4°C. Supernatant was removed and the pellet was dissolved in media, plated and incubated at 37°C with 5% CO<sub>2</sub>. On the 2<sup>nd</sup> day, considering the processing day as day 0, supernatant from the flask was collected and centrifuged at 1466xg for 4 minutes at 4°C. Supernatant was discarded and the pellet was plated in a fresh flask. Fresh media was added to the day 0 flask. Media of both flasks were changed again on the fourth and sixth day. The population of microglial cell were confirmed by staining them with *Ricinus communis* agglutinin-1 (RCA-1) lectin (Vector labs, FL-1081) (Jha, Srivastava et al. 2010). RCA stained cells were counted by blinded observers.

### 4.3.3 MTT ASSAY

10,000 BV2 microglia cell were seeded per well in a 96 well plate. Cells were pretreated with either 10mM N-acetyl-L-cysteine (NAC) for 3 hours or 10 $\mu$ M Cytochalasin D (CytoD) for 20 minutes and were incubated at 37°C with 5% CO<sub>2</sub>. After pretreatment cells were treated with 250 $\mu$ M, 500 $\mu$ M, 750 $\mu$ M, 1mM of DA for 24 hours. DA containing media was removed carefully from the microplate. 100 $\mu$ l of fresh serum free media and 10 $\mu$ l of MTT solution (Sigma) was added to each well. The plate was kept in incubator (Model 170S, Eppendorf) at 37°C with 5% CO<sub>2</sub> in dark for 2 hours. After incubation, 100 $\mu$ l of acidic isopropanol solution was added to each well and mixed thoroughly using pipette. Absorbance at 570nm was measured using a multi-mode microplate reader (Synergy H1 Hybrid, Biotek Instruments Inc).

### 4.3.4 IMMUNOCYTOCHEMISTRY

15,000 BV2 microglia cell seeded in each well of 2 well culture slides. Cells were pretreated with 10mM NAC for 3 hours, 10 $\mu$ M CytoD for 20 minutes, 10 $\mu$ M glyburide for 30 minutes or 10 $\mu$ M YVAD for 2 hours followed by treatment with mentioned concentration of DA or 24 hours. After treatment, cells were washed twice with 1X PBS for 5 minutes and were fixed for 10 minutes with 4% PFA. BV2 microglia cell were washed again twice and mounted with Fluoroshield with DAPI (Sigma-F6057). 15,000 primary adult human microglia cells were seeded in 2 well culture slides and treated with 2.5 $\mu$ M DA, LPS or 25nM PMA for 12 hours. 15,000 BV2 microglia cell were seeded in 2 well culture slides and treated with 250 $\mu$ M DA for 24 hours. After treatment, cells were washed twice with 1X PBS for 5 minutes and were fixed for 10 minutes with 4% PFA. Cells were washed again with 1X PBS and permeabilized with 0.1% TritonX-PBS for 15 minutes at room temperature. Further cells were blocked with 5% FBS in 0.1% TritonX-PBS for 1 hour in humidified chamber at 4°C and stained overnight in humidified chamber at 4°C with 1:1500 dilution of Anti-DNA/Histone H1 primary antibody (Merck, MAB3864) for primary cells and with 1:250 dilution of anti-Neutrophil Myeloperoxidase antibody (Sigma-Aldrich, N5787) for BV2 cells. After primary incubation, cells were washed and incubated for 1 hour with 1:500 dilution of anti-mouse or 1:1000 dilution of anti-rabbit secondary antibody. Cells were further washed and mounted with Fluoroshield with DAPI (Sigma-F6057). Images were taken using a fluorescence microscope (Leica Systems). Bright field images at 20X and 40X were taken on Nikon or Leica Microscope. Images were analyzed using ImageJ (Schneider, Rasband et al. 2012).

### 4.3.5 IMMUNOHISTOCHEMISTRY

We used 5- $\mu$ m sections embedded in paraffin that were deparaffinized and rehydrated through alcohols (Jha, Srivastava et al. 2010). The paraffin embedded paraformaldehyde fixed glioma (grade 4, Glioblastoma) and normal brain tissue were obtained with approval from the Internal Review Board and the Ethics Committees of AIIMS, Jodhpur and Tata Memorial Cancer Hospitals. Informed consent was acquired for the use of tissue samples for experiments from human participants. We have performed all experiments in accordance with the ethical guidelines and regulations of All India Institute of Medical Sciences Jodhpur and Indian Institute of Technology Jodhpur. For the detection of microglia, tissues were stained with 1:500 *Ricinus communis agglutinin-1* (RCA-1) lectin (Vector labs, FL-1081) (Jha, Srivastava et al. 2010). Glioma (paraformaldehyde fixed paraffin embedded grade IV glioblastoma) and normal brain (paraformaldehyde fixed paraffin embedded) tissue sections were stained for DNA/Histone H1 using 1:300 of anti- DNA/Histone H1 antibody (Merck) primary antibody and 1:500 anti-mouse secondary antibody. Nuclei were stained blue with DAPI. Immunofluorescence was observed using fluorescence microscope (Leica Systems) and analyzed using ImageJ (Schneider, Rasband et al. 2012).

#### **4.3.6 QUANTIFICATION OF EXTRACELLULAR TRAPS IN TISSUES**

5- $\mu$ m embedded paraffin sections of GBM and cerebrum were stained as described in immunohistochemistry section. The number of punctate structure with RCA, for microglia, and DNA/Histone H1, for ETs, overlap was quantified by the algorithm developed by us. The average of the quantified value was represented on the graph. Error bars represent standard error. The data is representative of two experiments.

#### **4.3.7 QUANTIFICATION OF EXTRACELLULAR TRAPS IN CULTURE SUPERNATANT**

The ETs in supernatant was quantified by measuring the fluorescence of digested traps (Joshi, Lad et al. 2013, Yoo, Floyd et al. 2014, Robledo-Avila, Ruiz-Rosado et al. 2018). 2,00,000 cells were seeded in 6 well plate. Cells were only dopamine or pretreated with 10 $\mu$ M glyburide for 30 minutes or 10 $\mu$ M YVAD for 2 hours followed by treatment with 250 $\mu$ M of dopamine and were incubated at 37°C with 5% CO<sub>2</sub> for 24 hours. Following incubation 10U/ml DNase I Solution (Himedia) was added to the wells and the plate was incubated at room temperature for 15 minutes. 5mM EDTA was added to the wells to stop the reaction. Supernatant was collected and centrifuged at 300g at room temperature. After centrifugation supernatant was transferred to clean centrifuge tubes. 200 $\mu$ l of supernatant was added to wells in a 96 well plate in duplicates. 5 $\mu$ M SYTOX™ Green Nucleic Acid Stain (Invitrogen) was added to the wells and the plate was incubated in dark for 15 minutes. The fluorescence was measured at excitation/emission = 485/530.

#### **4.3.8 EXTRACELLULAR TRAPS FUNCTIONAL ASSAY**

15,000 BV2 microglia cell seeded in 2 well chamber slides. After pretreatment with NAC or CytoD, as mentioned above, cells were treated with 250 $\mu$ M DA and incubated at 37°C with 5% CO<sub>2</sub>. FITC tagged *E. coli* taken from Vybrant Phagocytosis Assay Kit (V-6694), was added after 3 hours of addition of DA. Cells were further incubated at 37°C with 5% CO<sub>2</sub> for 21 hours. Cells were washed twice with 1X PBS for 5 minutes and were fixed with 4% PFA. Then they were washed again twice with 1X PBS for 5 minutes and were mounted with Fluoroshield with DAPI. Images were taken using a fluorescence microscope (Leica Systems)

#### **4.3.9 DETECTION OF ROS**

10,000 cells were seeded in 96 well microtiter plate and were incubated overnight at 37°C with 5% CO<sub>2</sub>. Cells were treated with 20 $\mu$ M of 2', 7'-Dichlorofluorescein diacetate (D6883 Sigma) for 30 minutes. Media was removed and the cells were washed once with 1X PBS. 100 $\mu$ l media was added to each well and cells were treated with 10mM NAC for 3 hours. Following this treatment cells were treated with 250 $\mu$ M DA for 24 hours. Fluorescence intensity indicating ROS generation was measured with a Synergy H1 Hybrid Multi-Mode reader (BioTek) at excitation and emission wavelength of 485/535 nm.

#### **4.3.10 ALGORITHM AND CODE FOR QUANTIFICATION OF EXTRACELLULAR TRAPS IN TISSUES**

There are three primary chromatic colors of light present in digital cell images. These are red (R), green (G) and blue (B). As we know, any digital color image consists of these three color channels and any other color is a combination of these three with different proportions (Koschan and Abidi 2008, Gonzalez and Woods 2018). We have utilized this basic property of digital color images while determining the overlapping between different regions. We have extracted out the three different color channels from the color image and processed those separately to determine the overlapped regions. That is, we perform a thresholding operation on each of the R, G and B images separately and carried out intersection operations between them.

Say,  $I$  is the colored cell image under consideration. In the other words, it can be said that  $I$  is a matrix of size  $MXNX3$ . Now, after extracting out three color channels there will be three different images each of size  $MXN$ . Let those be denoted as  $I_R, I_G$  and  $I_B$ . Let we set three threshold values  $T_R, T_G$  and  $T_B$  to extract out the regions with higher values of these three colors in the three images. The thresholding operation on  $I_R$  is carried out according to the equation given below.

$$B_R = \begin{cases} 1 & \text{if } I_R > T_R \\ 0 & \text{otherwise} \end{cases}$$

$B_R$  is the binarized image that we receive after performing thresholding on  $I_R$ . Please note, the pixels with value '1' in  $B_R$  represents the pixels with higher red component present in it. Similarly, we can have two more binarized images from  $I_G$  and  $I_B$  as  $B_G$  and  $B_B$  with thresholds  $T_G$  and  $T_B$  respectively.

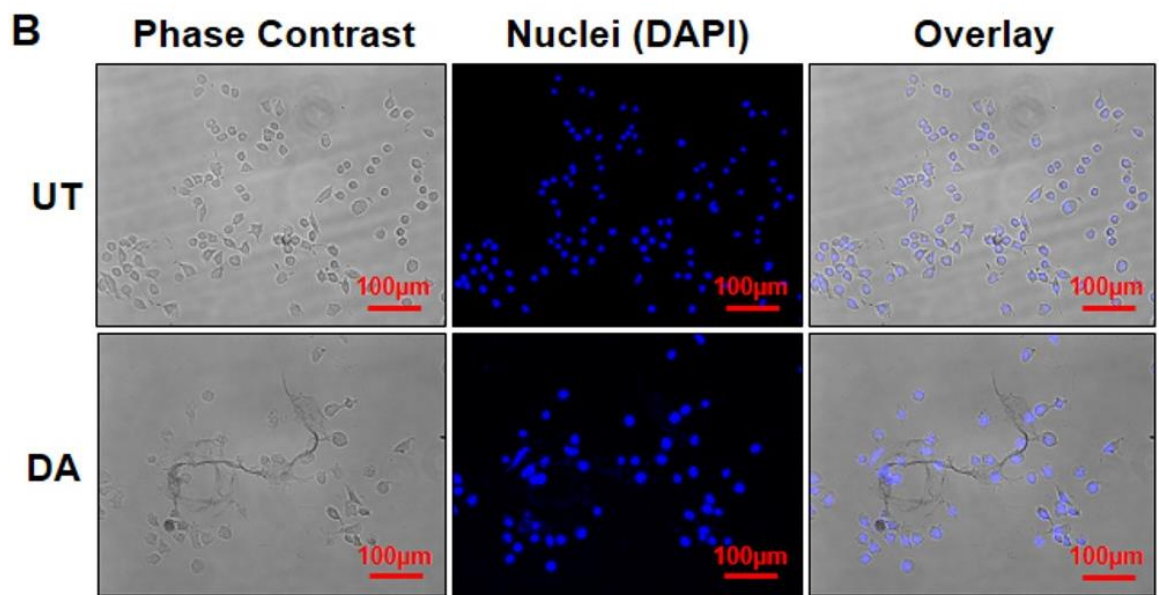
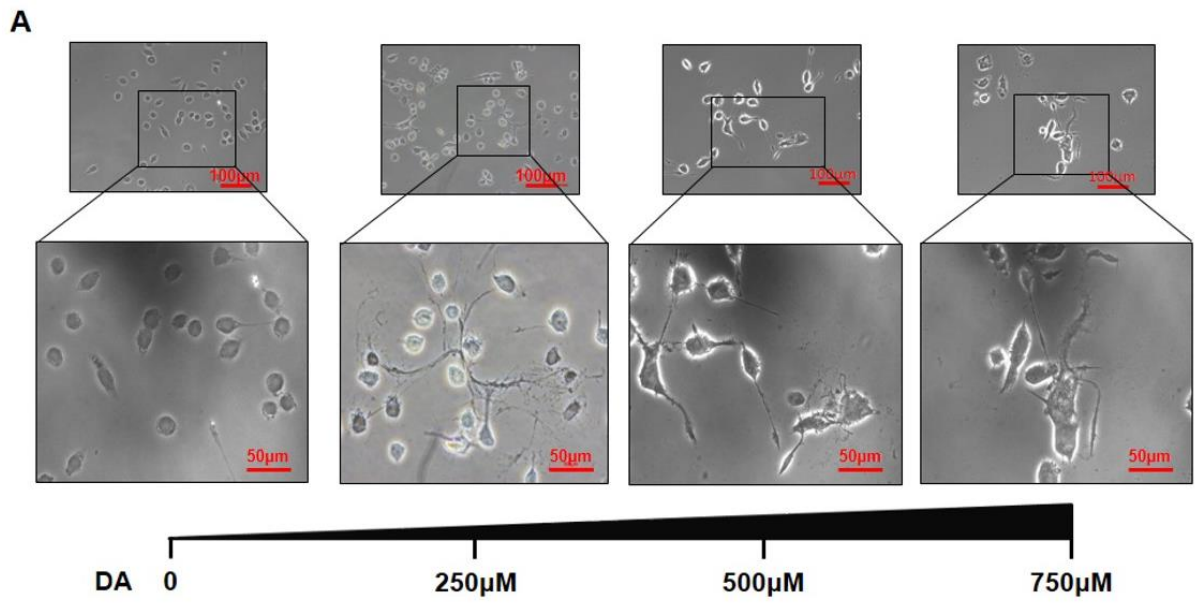
To determine the overlapped regions between red and green regions we perform  $B_R \cap B_G$ . The intersected region will reflect the overlapped areas of red and green regions in the cell image. The same will be performed between  $B_G \cap B_B$ , and  $B_R \cap B_B$  to determine the green-blue and red-blue overlapped regions.

Further, we have eliminated the noisy regions those were present in the intersected image. We have considered the small regions as noise and eliminated them. The small regions are chosen to be of 10% of size of the largest region that is present in the intersected image. The remaining regions will finally be labelled as the overlapped regions.

## 4.4 RESULTS AND DISCUSSION

### 4.4.1 DOPAMINE INDUCES FORMATION OF EXTRACELLULAR TRAPS IN MICROGLIA

Presence of DA receptors on microglia and cells of adaptive and innate immune system points towards DA's role in immune regulation (Sookhai, Wang et al. 1999, McKenna, McLaughlin et al. 2002, Pocock and Kettenmann 2007). We started with examining whether DA induces ETs formation in BV2 microglia cell line. We treated the cells with different concentrations of DA for 24 hours. All the concentrations of DA induced traps like structures in BV2 microglia cell as visualized by phase contrast microscopy (Figure 4.1A). DA concentration varies in different regions of brain and can increase up to  $1800\mu\text{M}$  (Ewing, Bigelow et al. 1983, Olefirowicz and Ewing 1990, Basu, Nagy et al. 2001, Lucas and McMillen 2002, Goto, Otani et al. 2007, Yan, Jiang et al. 2015, Matt and Gaskill 2020). We used  $250\mu\text{M}$  of DA for further experiments. ETs are composed of decondensed chromatin and hence they are stained by DAPI. Antimicrobial protein MPO is also embedded on ETs. We stained the DA induced traps like structures with DAPI (Figure 4.1B, C) and MPO that confirmed their identity as ETs. We further quantified the presence of ETs in the culture supernatant by digesting them with DNase I which showed that DA was inducing ETs in BV2 microglia cell line (Figure 4.1D).



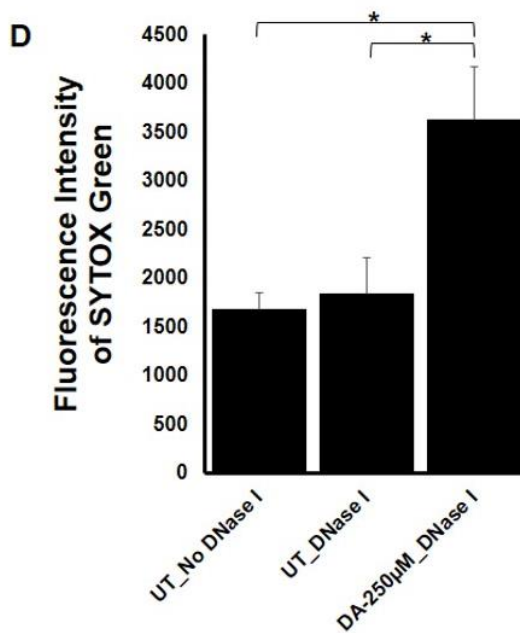
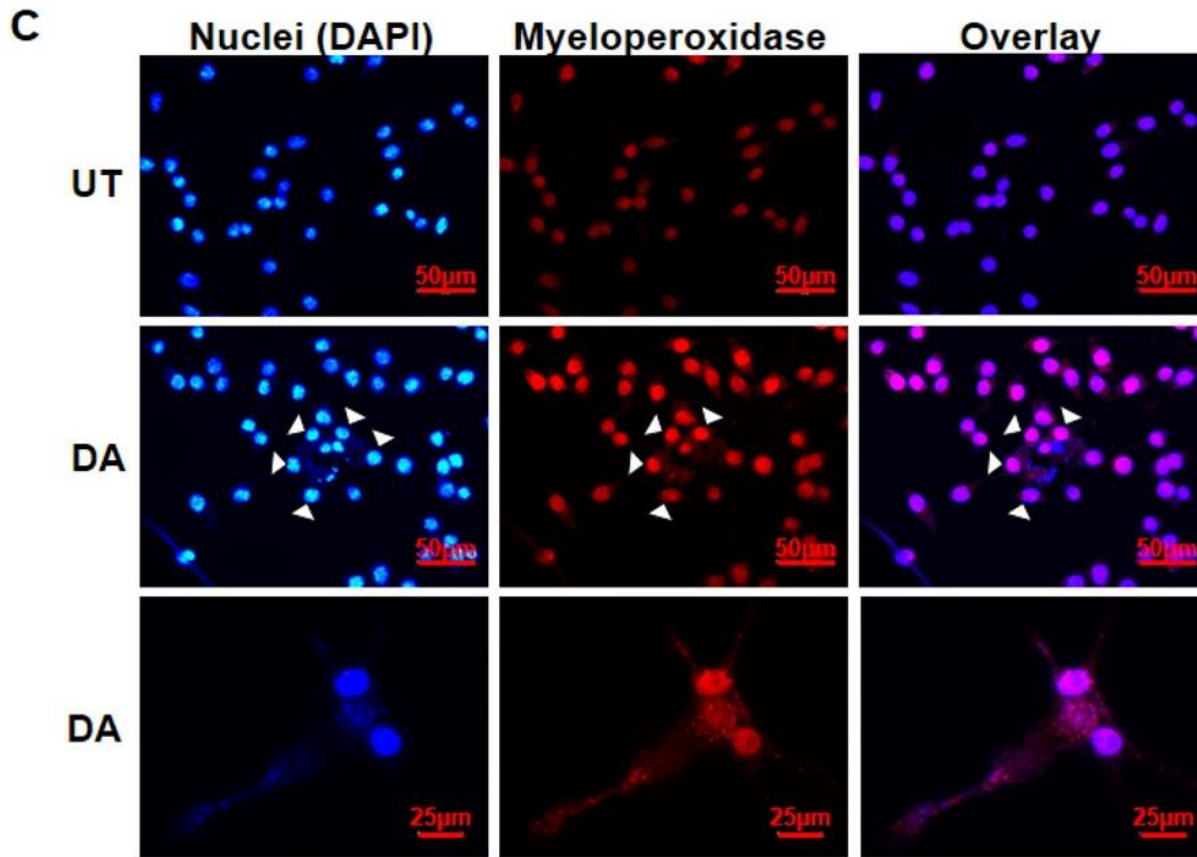


**Figure 4.1 :** Visualization of DA Induced Extracellular Traps in BV2 Microglia. (A) BV2 microglia were incubated with different concentrations of Dopamine (DA) for 24 hours. ETs were clearly visible at all the concentrations of DA. Scale bars, 100µm and 50µm. (B), (C) BV2 microglia were incubated with 250µM of DA for 24 hours. ETs were stained with just DAPI (blue) (B) or DAPI and MPO (C). The images are representative of three experiments. At least 7 frames were imaged per well in a two well chamber slide. Scale bars, 100µm, 50µm and 25µm. (D) DNase I was added after 24 hours in DA treated wells and untreated (UT) wells. Fluorescence was measured in the collected supernatant with the help of SYTOX™ Green. Graph is representative of 4 experiments. Data represented as mean +/- SEM. \* $p < 0.05$  (Student's t-test).



#### 4.4.2 EXTRACELLULAR TRAPS ARE BEING FORMED INDEPENDENT OF CELL DEATH

Cells forming ETs via suicidal NETosis pathway die immediately while cells following vital NETosis pathway survive and continue to function normally (Yipp and Kubes 2013, Papayannopoulos 2017). We next performed MTT assay to determine whether ETs are induced by lytic ETosis or vital ETosis (Figure 4.2). DA did not cause significant cell death at any concentration. This confirmed that DA induced BV2 microglia cell are following vital ETosis. Yousefi et al. first showed that neutrophils can survive even after the formation of NETs. Interestingly the traps formed by viable neutrophils contained mitochondrial DNA instead of nuclear DNA (Yousefi, Mihalache et al. 2009). How long does microglia survive after expelling its DNA and what is the composition of microglia ETs are intriguing areas for future investigations. To investigate the mechanism of ETs formation in BV2 cells we have used NAC (N-Acetyl-L-cysteine), an antioxidant, and Cytochalasin D (CytoD), an actin polymerization inhibitor, along with DA in our experiments. We checked the cytotoxicity of NAC and CytoD along with DA on BV2 microglia cell. NAC and DA did not cause significant cell death while CytoD and DA were toxic to cells.

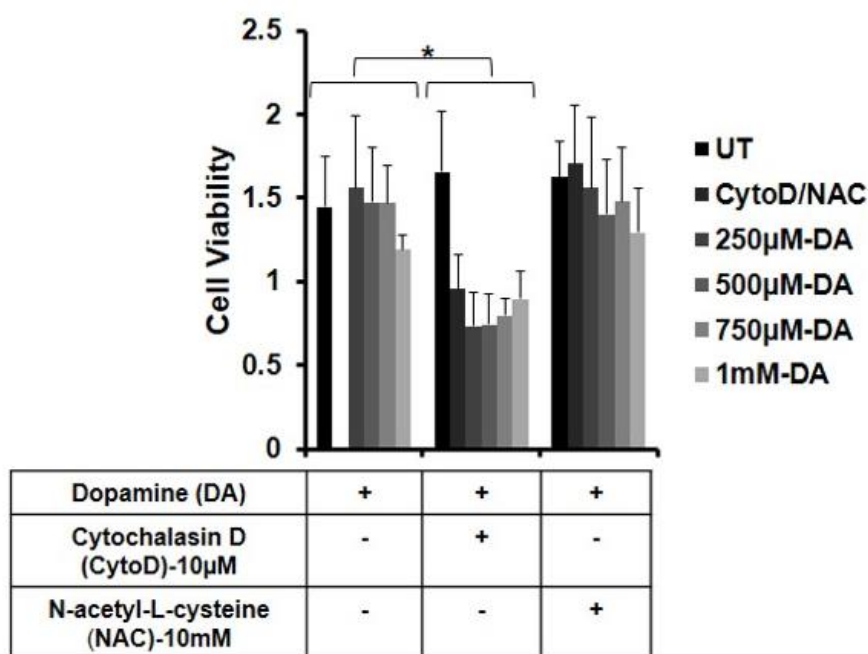
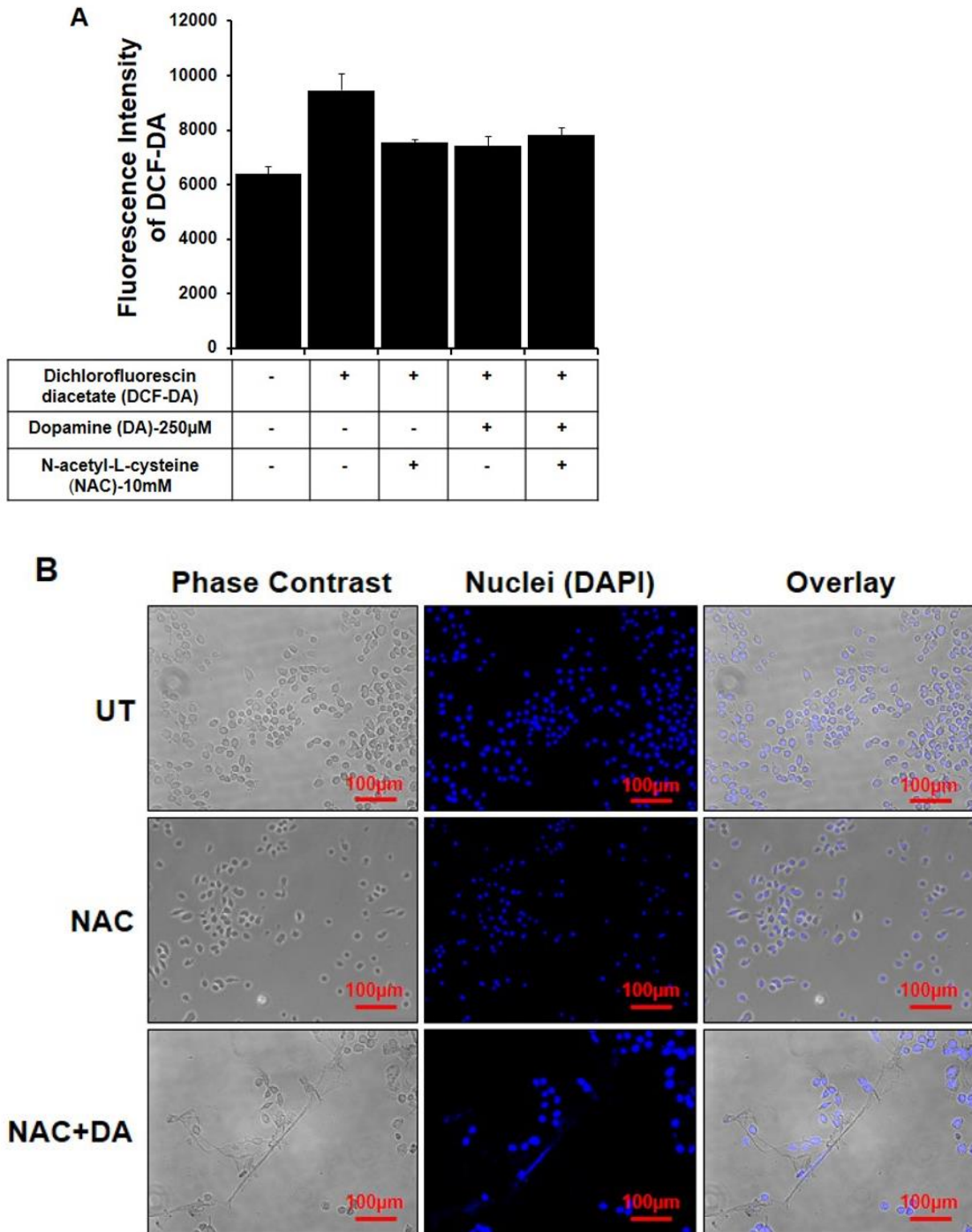


**Figure 4.2 :** Dopamine Induces Extracellular Traps Formation Independent of Cell Death. BV2 microglia were seeded in 96 well microplate and were pretreated with 10µM Cytochalasin D (CytoD) for 20 minutes and 10mM N-acetylcysteine (NAC) for 3 hours. Pretreatment was followed by Dopamine (DA) treatment for 24 hours. Cell viability was observed by taking the absorbance at 570 nm. The graph is representative of 3 experiments. Data represented as mean +/- SEM. \*p<.05 (Student's t-test).

#### 4.4.3 MICROGLIA FORM EXTRACELLULAR TRAPS IN ROS INDEPENDENT MANNER

Formation of ETs are ROS dependent and/or independent (Papayannopoulos 2017). To examine which pathway contributes to ETs formation in BV2 microglia, we inhibited ROS production by pretreating the cells with NAC and confirmed the inhibition by Dichlorofluorescein diacetate (DCF-DA) (Figure 4.3A). DA can work as an antioxidant (Jodko-Piórecka and Litwinienko 2015) and our results showed that DA did not induce significant ROS generation in BV2 microglia (Figure 4.3A), hence NAC did not have significant effect on the level of ROS. This

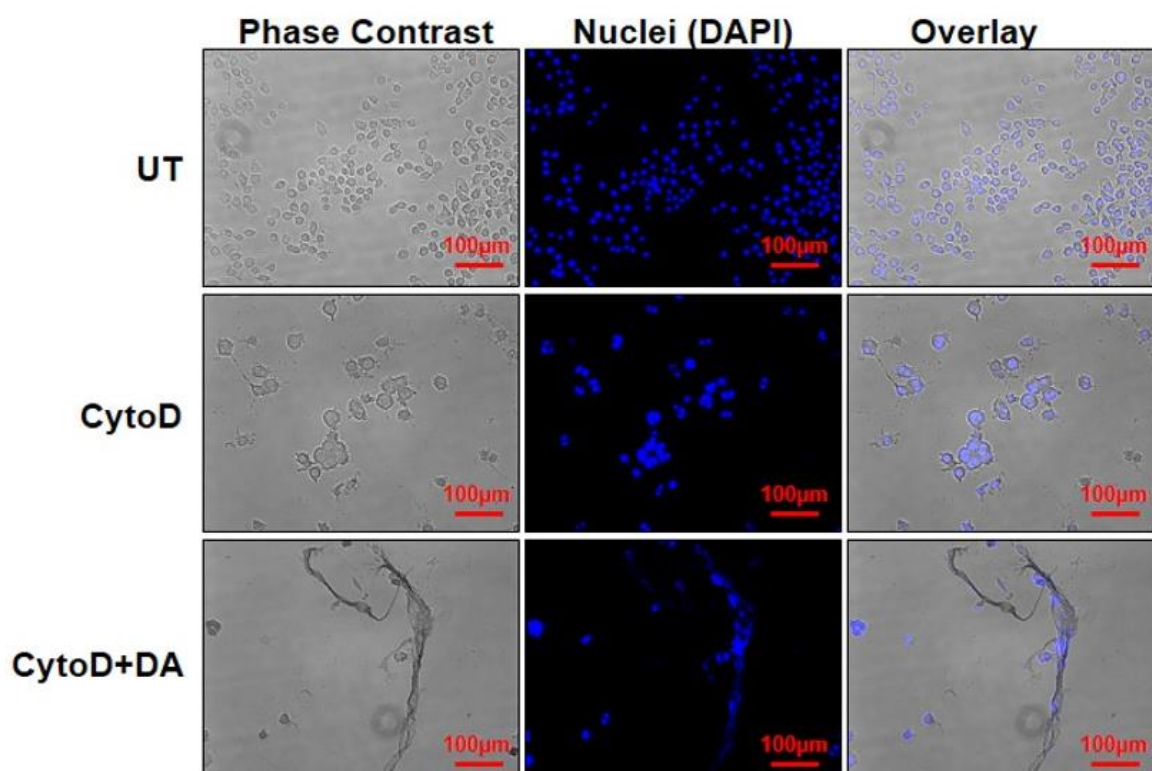
result suggests that DA induces ETs in a ROS independent manner. To confirm this finding we treated ROS inhibited BV2 cells with DA and observed ETs formation. Inhibition of ROS did not inhibit the formation of DA induced ETs as evident from immunofluorescence images (Figure 4.3B). These results confirmed that DA induces ETs formation in BV2 microglia cell via ROS independent pathway. ROS independent ETs formation are previously reported to follow vital ETosis (Pilszczek, Salina et al. 2010). The molecules involved in this pathway are under-explored. ETs formation is highly stimulus dependent (Doster, Rogers et al. 2017, Papayannopoulos 2017, Daniel, Leppkes et al. 2019). Our result is crucial, as evidence of different stimuli inducing vital ETosis will help in exploring molecular pathways.



**Figure 4.3 :** *Dopamine Induces Extracellular Traps Independent of ROS.* Cells were pretreated with 10mM N-acetylcysteine (NAC) for 3 hours followed by 250 $\mu$ M Dopamine (DA) treatment for 24 hours. (A) ROS production was checked with the help of Dichlorofluorescein diacetate (DCF-DA). The graph is representative of three experiments. Data represented as mean  $\pm$  SEM. (B) ETs formation was induced by DA even in the presence of NAC. ETs were stained with DAPI (blue). At least 7 frames were imaged per well. Scale bars, 100 $\mu$ m.

#### 4.4.4 EXTRACELLULAR TRAPS FORMATION IN BV2 MICROGLIA CELL IS INDEPENDENT OF ACTIN POLYMERIZATION

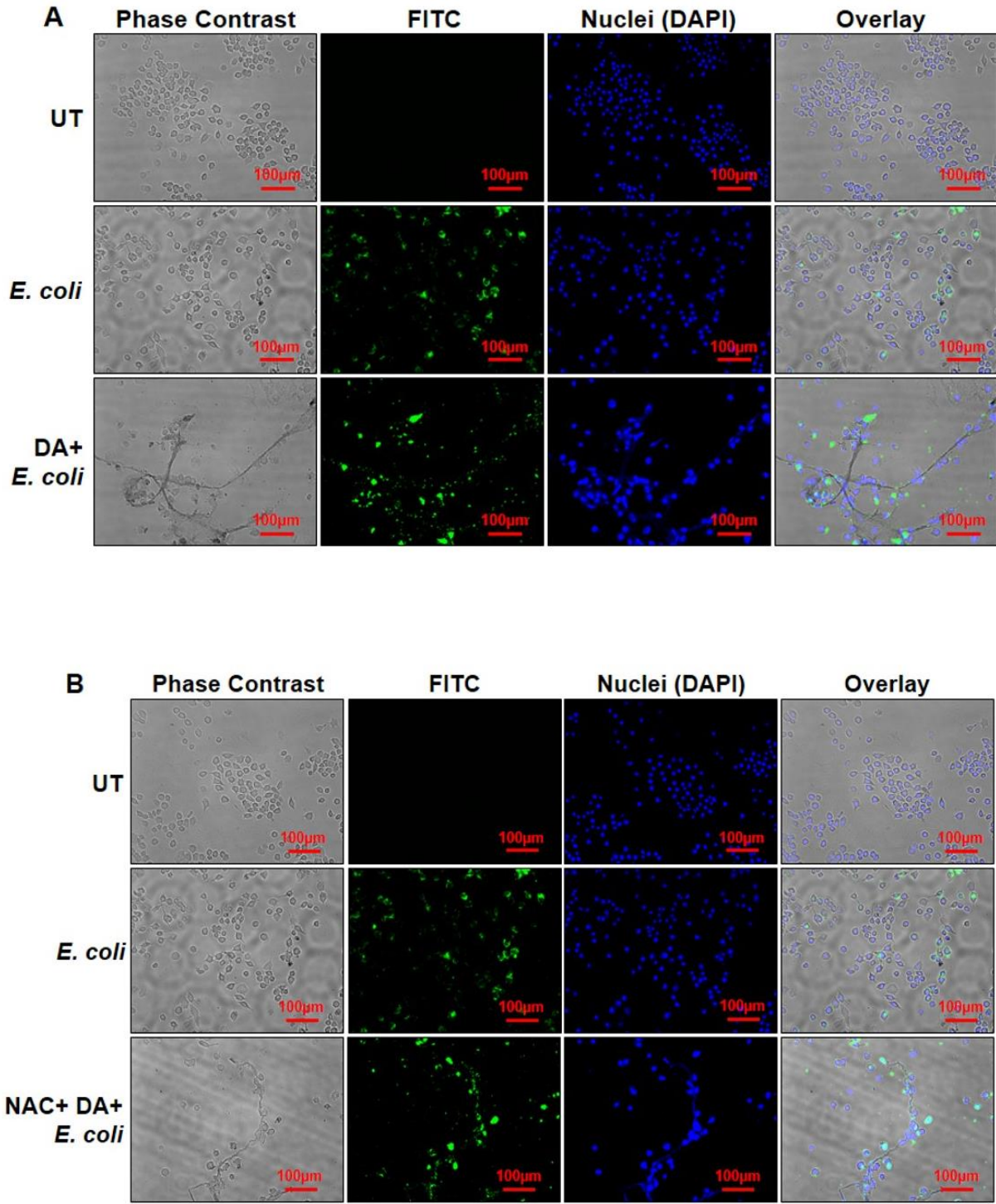
Actin dynamics may play a role in the formation of ETs (Metzler, Goosmann et al. 2014). But sometimes inhibition of actin polymerization does not affect ETs formation (Abi Abdallah, Lin et al. 2012, Granger, Faille et al. 2017). To investigate whether actin polymerization plays a role in ETs formation in microglia, we preincubated BV2 cells with CytoD and then treated them with DA (Figure 4.4). Immunofluorescence images confirmed that DA induced ETs formation independent of actin polymerization, but the viability of cells was significantly reduced – also seen in MTT assay (Figure 4.2). This indicates that CytoD and DA treated BV2 cells may follow lytic ETosis. ETs are hypothesized as an alternate mechanism adopted by immune cells to counter pathogens when their phagocytic capacity is overwhelmed (Branzk, Lubojemska et al. 2014). It is possible that in some cases inhibiting phagocytosis might push immune cells towards ETs inducing pathways.

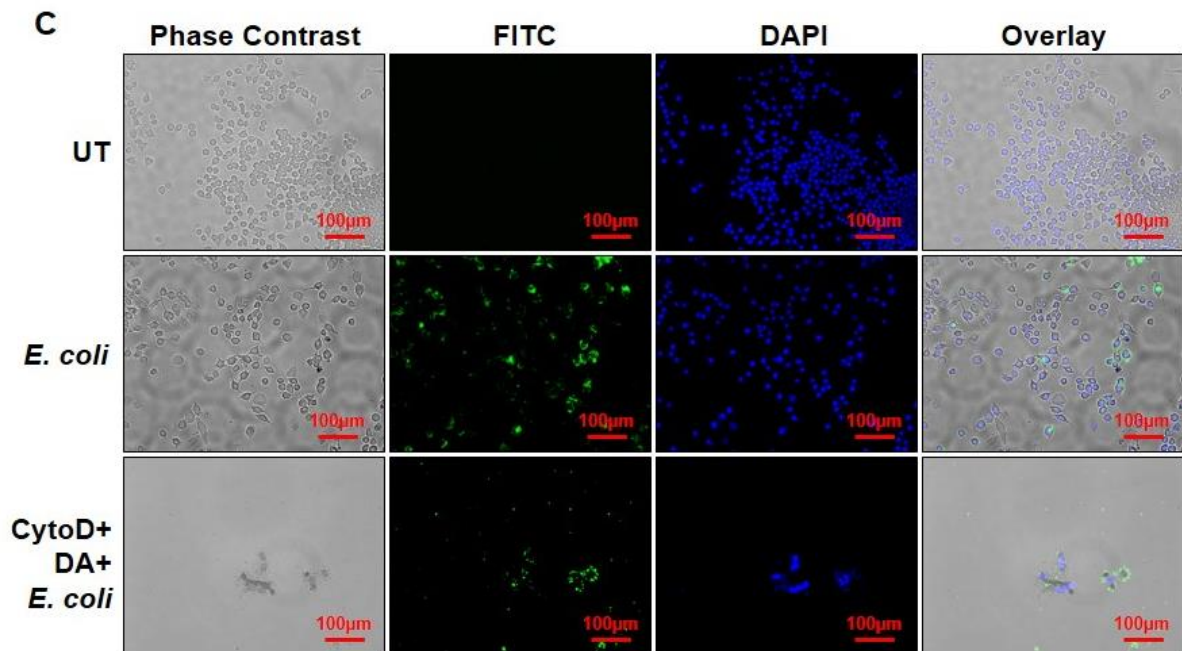


**Figure 4.4 :** *Extracellular Traps Formation is Independent of Actin Polymerization.* Cells were pretreated for 20 minutes with 10 $\mu$ M Cytochalasin D (CytoD) followed by treatment with 250 $\mu$ M Dopamine (DA) for 24 hours. Inhibition of actin polymerization had no effect on ET formation. ETs were stained with DAPI (blue). The images are the representative of two experiments. At least 7 frames were imaged per well. Scale bars, 100 $\mu$ m.

#### 4.4.5 DOPAMINE INDUCED EXTRACELLULAR TRAPS ARE FUNCTIONAL

One of the key functions of ETs is to trap pathogens (Brinkmann, Reichard et al. 2004, Doster, Rogers et al. 2017, Papayannopoulos 2017). We further investigated whether DA induced BV2 microglia ETs are functional and can trap bacteria. We incubated FITC tagged *E. coli* with BV2 cells treated with only DA, NAC+DA or CytoD+DA (Figure 4.5A, B, C). Immunofluorescence microscopy images confirmed that DA induced ETs are functional and capture *E. coli*. NAC had no effect on the functionality of traps, however CytoD reduced the functionality of traps (Figure 4.5C).

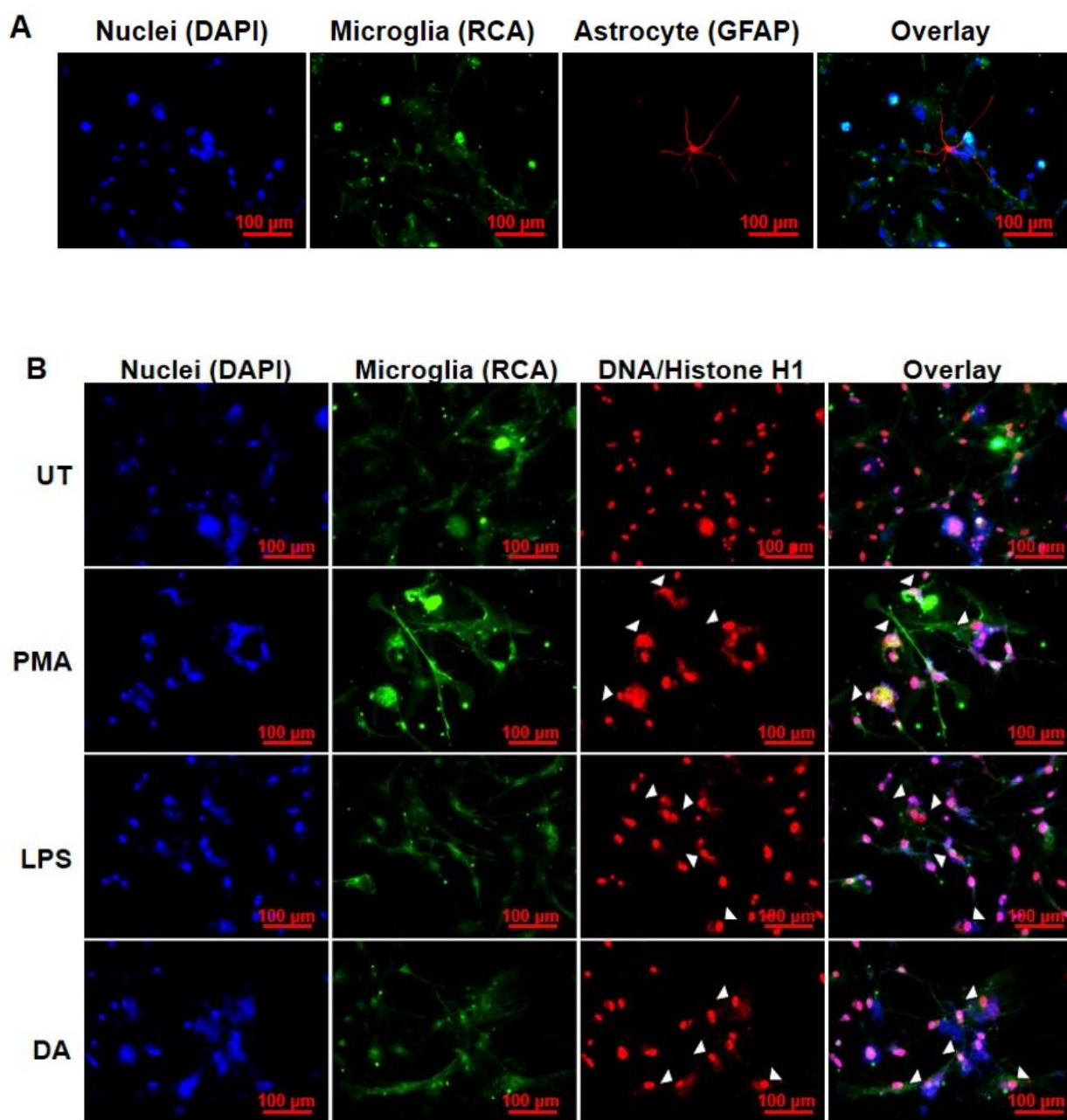




**Figure 4.5 :** Dopamine Induces Formation of Functional Extracellular Traps. (A) (B) (C) BV2 microglia were pretreated with N-acetylcysteine (NAC) or cytochalasinD (CytoD) and were incubated with Dopamine (DA) for 3 hours. FITC tagged *E. coli* (green) was added followed by DA incubation and cells were further incubated for 21 hours. ETs were stained with DAPI (blue). In the overlay image green dots are overlapping with the blue ETs suggesting that ETs are trapping *E. coli*. Images are representative of two experiments. At least 7 frames were imaged per well. Scale bars, 100µm.

#### 4.4.6 DOPAMINE INDUCES EXTRACELLULAR TRAPS IN PRIMARY HUMAN MICROGLIA

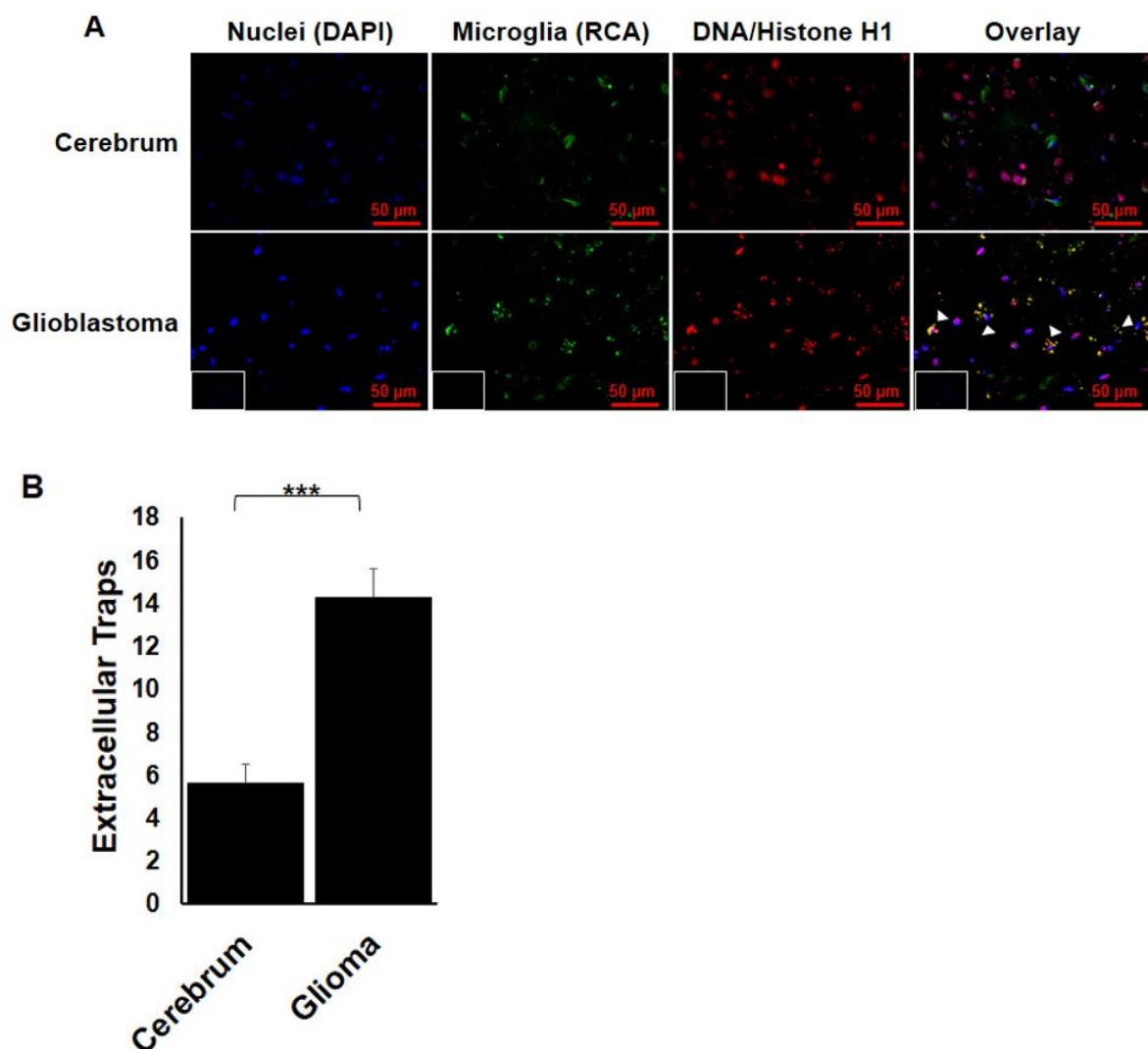
It was clear from our results that DA induces functional ETs in BV2 microglia cell line. We extended our investigation to primary adult human microglia. We isolated primary adult human microglia, as described previously (Agrawal, Saxena et al. 2020), and characterized them by staining with *Ricinus communis agglutinin* (RCA) and GFAP (Figure 4.6A). To determine whether DA can induce ETs in primary human microglia, we treated the isolated cells with 2.5µM DA and other known ETs inducers, PMA and LPS (Doster, Rogers et al. 2017, Papayannopoulos 2017) for 12 hours (Figure 4.6). We stained the cells with RCA (green), as a microglial marker as well as DAPI (Blue) and anti-DNA/Histone H1 antibody (Red) for ETs (Figure 4.6D). Immunofluorescence images confirmed that DA induces ETs in primary human microglia. This was exciting and it opened new avenues of microglia ETs exploration. PMA and LPS induce ETs in different cells primarily via ROS dependent lytic pathway (Fuchs, Abed et al. 2007, Khan, Farahvash et al. 2017) while our results in BV2 cells suggest a ROS independent non-lytic pathway for microglia ETs formation. Our results support the heterogeneity of ETs formation pathway adopted by cells depending on the stimuli (Pieterse, Rother et al. 2016, Daniel, Leppkes et al. 2019, Petretto, Bruschi et al. 2019).



**Figure 4.6 : Dopamine Induces Extracellular Traps in Primary Human Microglia.** (A) Primary human microglia isolated from adult human brain tissues. RCA (Green) was used as microglia marker and GFAP (Red) was used as astrocyte marker. About 80% of the cells isolated were microglia. (B) Isolated microglia were treated with 2.5 $\mu$ M Dopamine (DA) for 12 hours. RCA (Green) was used as microglia marker. ETs (Arrow heads) were visualized using DAPI (Blue) and DNA/Histone H1 antibodies (Red). At least 7 frames were imaged per well of the two well chamber slide. Scale bars, 100 $\mu$ m.

#### 4.4.7 MICROGLIA EXTRACELLULAR TRAPS ARE PRESENT IN GLIOBLASTOMA

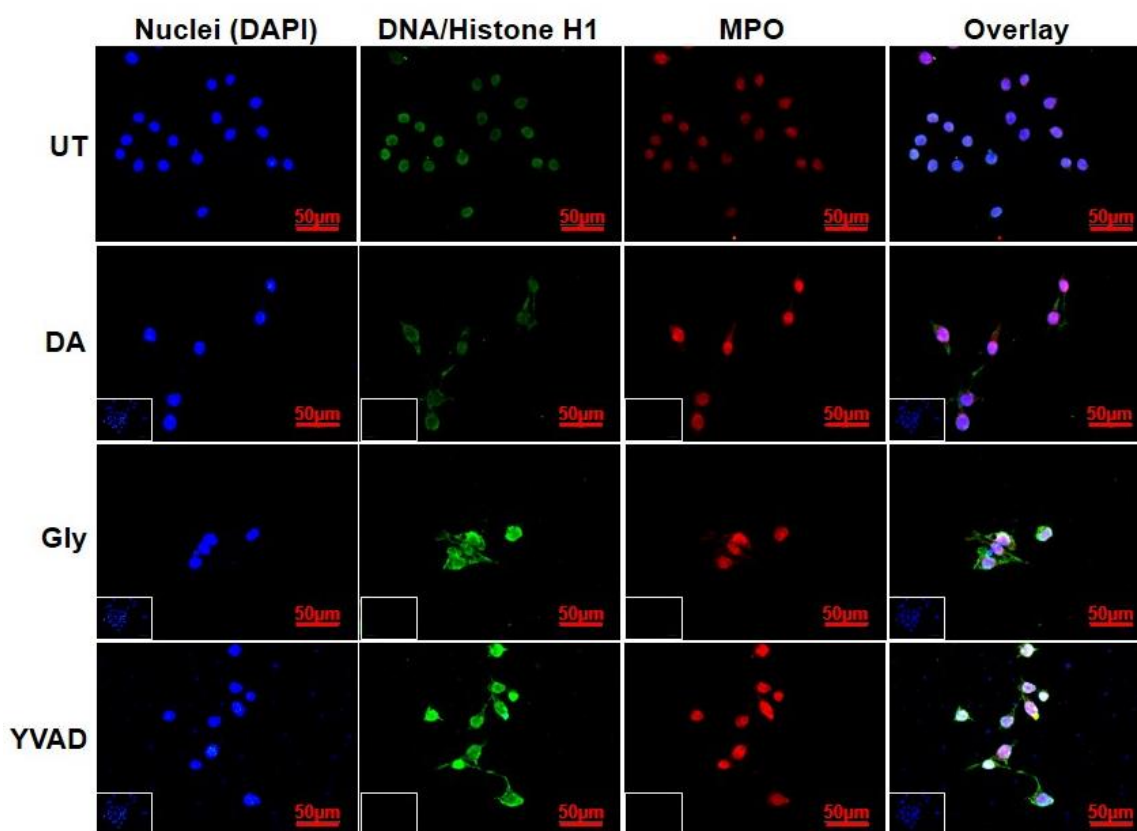
Recent studies suggest that GBM cells express DR2 and secrete DA (Caragher, Shireman et al. 2019, Weissenrieder, Reed et al. 2019). This may increase local concentration of DA within the tumor microenvironment which is yet to be quantified. These findings encouraged us to investigate whether microglia present in the GBM microenvironment form extracellular traps. We stained GBM tissues with RCA for microglia (green) and H1/DNA antibody for ETs (Red). H1/DNA staining was uniformly distributed inside the cells' nucleus in human cerebrum tissue. Whereas it showed a punctate staining around the cells in case of GBM tissues (Figure 4.7). Overlap of H1/DNA and RCA confirmed the formation of ETs by microglia. An algorithm was developed to quantify the formation of ETs. GBM tissues showed significant formation of ETs. There are cells other than microglia that are also showing punctate stain. This may be because of the presence of neutrophils and other cells within GBM tissue (Chen and Hambardzumyan 2018, Schiffer, Annovazzi et al. 2018) that are known to form ETs. ETs play a role in metastasis of cancer and cancer cells in turn can induce ETs (Cools-Lartigue, Spicer et al. 2013, Park, Wysocki et al. 2016, Tohme, Yazdani et al. 2016). It is necessary to explore if that is true for GBM.



**Figure 4.7 :** Presence of Microglia Extracellular Traps in GBM. (A) GBM tissue was stained with DAPI (Blue), RCA (Green) for microglia and DNA/Histone H1 (Red) for ETs. The formation of ETs by microglia can be visualized by the punctate red staining overlapping with green (Arrow heads). Inset represents secondary antibody control. Scale bars, 50µm. (B) The punctate red staining overlapping with green was quantified. The graph represents average of the quantified value. The result is representative of two experiments. At least 7 frames were imaged per section and quantified. Data represented as mean +/- SEM. \*\*\* $p < .0001$  (Student's t-test).

#### 4.4.8 NLRP3 REGULATES MICROGLIA ETs FORMATION

Since intracellular LPS induces NETs through noncanonical activation of NLRP3, caspase-11 and gasdermin D, we checked whether NLRP3 or caspase-1 are involved in microglia ET formation (Chen, Monteleone et al. 2018). We pretreated BV2 microglia with glyburide (Gly) for NLRP3 inhibition and YVAD for caspase-1 inhibition followed by DA treatment. Interestingly inhibiting either of them did not inhibit ETs formation (Figure 4.8A). We further quantified the presence of traps in supernatant by digesting them with DNase I. To our surprise inhibiting NLRP3 further increased DA induced microglia ETs formation in BV2 cells (Figure 4.8B). NLRP3 has been reported to play a role in NETs formation (Chen, Monteleone et al. 2018). In turn NETs have also been reported to induce NLRP3 inflammasome in case of lupus (Kahlenberg, Carmona-Rivera et al. 2013). The role of inflammasome components in regulating innate immune functions along with inflammation has been reported earlier. NLRP3 inflammasome gets secreted out of macrophages and functions as DAMP to induce inflammation (Baroja-Mazo, Martín-Sánchez et al. 2014). NLRP3 depletion increase phagocytosis in BV2 microglia cells (Schölwer, Habib et al. 2020). Similarly astrocytes heterozygous for ASC (ASC<sup>+/-</sup>) show an increase in phagocytosis when compared to astrocytes from wild type and ASC<sup>-/-</sup> mice (Couturier, Stancu et al. 2016). Dependence or independence of ETs formation on phagocytosis is a matter of debate. Some studies suggest that inhibiting phagocytosis might enhance ETs formation as an alternate immune mechanism, some suggests that it may inhibit ETs formation (Schorn, Janko et al. 2012, Yousefi, Morshed et al. 2015, Je, Quan et al. 2016). Phagocytosis and microglia ETs formation needs in depth exploration. NLRP3 might also regulate trap formation via other mechanism which needs to be studied.





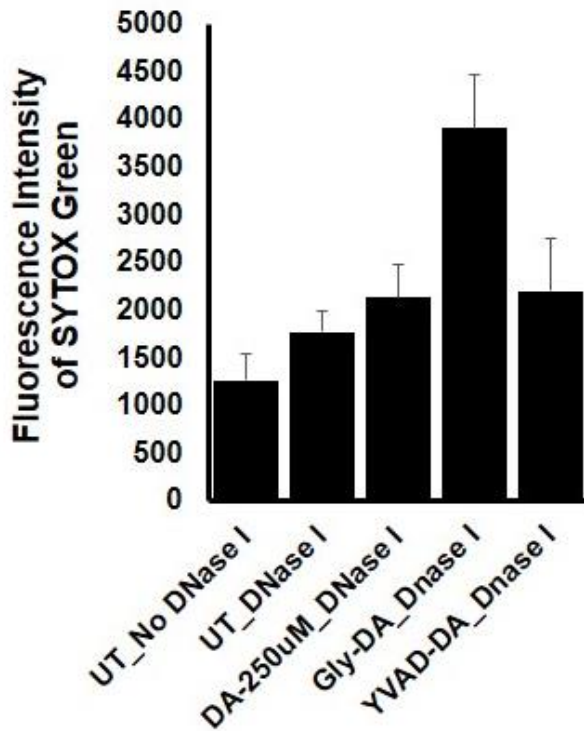


**Figure 4.8** NLRP3 regulates microglia ETs formation: BV2 Cells were pretreated with 10 $\mu$ M glyburide (Gly) for 30 minutes or 10 $\mu$ M YVAD for 2 hours followed by 250 $\mu$ M Dopamine (DA) treatment for 24 hours. (A) ETs were stained with DNA/Histone H1 antibodies (Green) and MPO (Red) (C). The images are representative of two experiments. At least 7 frames were imaged per well in a two well chamber slide. Scale bars 50 $\mu$ m. (B) DNase I was added to wells after 24 hours of DA treatment. Fluorescence was measured in the collected supernatant with the help of SYTOX™ Green. Graph is representative of 4 experiments. Data represented as mean  $\pm$  SEM. \* $p$ <0.05 (Student's t-test).

#### 4.5 CONCLUDING REMARKS

Dopamine (DA) plays many roles in the brain, especially in; movement, motivation, and reinforcement of behavior, however, its role in regulating innate immunity is not clear. Here we have shown that dopamine can induce DNA based extracellular traps in primary, adult, human microglia and BV2 microglia cell line. These DNA based extracellular traps are formed independent of reactive oxygen species, actin polymerization and cell death. Inhibition of NLRP3 increased the traps formation. This indicates that NLRP3 may play central role in DA induced microglia extracellular traps. These traps are functional and capture FITC tagged *Escherichia coli* even when reactive oxygen species production or actin polymerization are inhibited. We confirmed the presence of microglial extracellular traps in *Glioblastoma multiforme* and developed an algorithm to quantify it. This is crucial because *Glioblastoma multiforme* cells are known to secrete dopamine. Our findings demonstrate that dopamine plays a significant role in sterile neuro-inflammation by inducing microglia extracellular traps.

